agronomy

MDPI

Article

Estimation of the Weight and Volume of Lime (*Citrus aurantifolia* (Christm.) Swingle) Fruit Using Computer Vision Based on Traditional Machine Learning and Deep Learning

Jiraporn Onmankhong [1], Pasu Poonpakdee [2] and Ravipat Lapcharoensuk [1,*]

[1] Department of Agricultural Engineering, School of Engineering, King Mongkut's Institute of Technology Ladkrabang, Bangkok 10520, Thailand; jiraporn.on@kmitl.ac.th
[2] Department of Industrial Engineering, School of Engineering, King Mongkut's Institute of Technology Ladkrabang, Bangkok 10520, Thailand; pasu.po@kmitl.ac.th
* Correspondence: ravipat.la@kmitl.ac.th

Abstract: The post-harvest process is important to increasing the market value of limes and requires focus. During this process, limes are graded and categorized based on size, weight, and volume. Therefore, identifying efficient means of estimating these properties is very important and remains an open research area. This study applies the concept of computer vision based on traditional machine learning algorithms (partial least square regression (PLS), epsilon-support vector regression (ε-SVR), decision tree (DT), random forest (RF), adaptive boosting (AB), gradient boosting (GB), Bagging meta-estimator (BME), and extremely randomized trees (ERTs)) and pre-trained deep learning (InceptionV3, MoblieNetV2, ResNet50, and VGG-16) for estimating the weight and volume of limes. Our findings showed that the BME and ResNet50 could yield the highest performance for estimating the weight and volume of limes. The BME produced R^2_{test} values of 0.954 and 0.882 for weight and volume, respectively, while the R^2_{test} values of ResNet50 models were between 0.951 and 0.957 for weight and volume, respectively. This study concluded that computer vision based on both traditional machine learning and deep learning could be used to estimate the weight and volume of limes. The approach proposed in this study can be adopted for applications related to computer vision in the post-harvest process.

Keywords: lime; weight; volume; computer vision; machine learning; deep learning

Citation: Onmankhong, J.; Poonpakdee, P.; Lapcharoensuk, R. Estimation of the Weight and Volume of Lime (*Citrus aurantifolia* (Christm.) Swingle) Fruit Using Computer Vision Based on Traditional Machine Learning and Deep Learning. *Agronomy* **2024**, *14*, 2434. https://doi.org/10.3390/agronomy14102434

Academic Editor: Yanbo Huang

Received: 30 August 2024
Revised: 4 October 2024
Accepted: 17 October 2024
Published: 20 October 2024

1. Introduction

Citrus fruits are sources of essential nutrients, namely glycemic and nonglycemic carbohydrates (sugars and fiber), potassium, folate, calcium, thiamin, niacin, vitamin B6, phosphorus, magnesium, copper, riboflavin, pantothenic acid, and a variety of phytochemicals [1]. The citrus fruit lime (*Citrus aurantifolia* (Christm.) Swingle) is a high-priority crop in many countries around the world. Although the fruit originated in Southeast Asia, it is now found in tropical and subtropical regions worldwide [2]. The physical properties of limes, including shape, size, weight, and volume, are important for determining juice yield, fruit consistency, the regulation of wholesale and retail prices, and consumer acceptance. These properties are the most essential indicators for designing and optimizing post-harvest machinery, including equipment used for cleaning, grading, conveying, processing, packaging, and transportation. Currently, limes are graded based on their size so that the process can be carried out using various methods, including manual labor and sorting machinery. Nevertheless, manual labor is not efficient; it is time-consuming, inefficient, and labor-intensive, and traditional sorting machinery is limited in its ability to accommodate various lime standards in different regions [3]. Typically, the size, weight, and volume of lime have shown some degree of correlation [4]. The weight and volume of fruits are important indicators for developing applications for quality evaluation, packaging,

transportation, and marketing. Currently, weight measurements are performed manually by weighing each individual lime. To measure volume, the water displacement method (WDM), in which a product is fully immersed in water and the increase in water level is taken as the volume of the product, is the most conventional approach [5]; however, these procedures are also time-consuming, inefficient, labor-intensive, and susceptible to error and therefore unsuitable for adoption on an industrial scale. Therefore, an effective, rapid, non-destructive, and reliable method for estimating size, weight, and volume is critical for enhancing automation in the post-harvest process and the commercial value of limes.

In recent years, computer vision (CV) has been widely adopted in agriculture, particularly in the post-harvest process, to decrease both machine costs and human errors. CV is a robust, powerful, and non-destructive method for assessing physical properties, including color, size, shape, weight, volume, and so on, which requires image analyses, image processing, and machine learning (ML) procedures. In previous research, several feature extraction methods with traditional ML regression algorithms, namely linear regression (LR), multiple linear regression (MLR), support vector regression (SVR), and artificial neural networks (ANNs), were applied to estimate the weight and volume of fruit. A traditional algorithmic system is highly mature, and it can be applied to estimate the weight and volume of fruit. Calixto et al. (2019) reported the application of an LR model to predict the weight of yellow melon [6]. The LR model was created using an area of yellow melon fruit which was extracted from an image using the Otsu threshold algorithm. The result showed that the LR model could predict the weight of yellow melon with a Pearson's correlation of 0.989. The estimation of the volume and weight of tomatoes using computer vision and machine learning algorithms was studied by Nyalala et al. (2019) [7]. SVR with various kernel functions (linear, quadratic cubic, and radial basis function (RBF)) and ANN algorithms was established using 2D (area, perimeter, major and minor axis lengths, eccentricity, and radial distance), and 3D (surface area and volume) shape indicator forms. The RBF-SVR outperformed all the explored models, with R^2 values of 0.9706 and 0.9694 for predicting weight and volume, respectively. Continuous research on estimating the weight and volume of single and occluded tomatoes using machine vision was proposed by Nyalala et al. (2021) [5]. Seven ML techniques, including SVR with different kernel functions (i.e., linear, cubic, quadratic, and RBF) and ANNs with three weight optimization algorithms (i.e., Levenberg–Marquardt, Bayesian regularization, and scaled conjugate gradient training algorithms), were adopted for developing models. The Bayesian regularization ANN was the highest-performance model, which could predict the weight and volume of tomato with R^2 values of 0.971 and 0.982, respectively. The study focused on estimating the weight and volume of Thai apple berries via computer vision, in which MLR and linear SVR algorithms were developed based on model predictions of physical properties (length, diameter, perimeter, or projected area) from fruit images [8]. The linear SVM model showed that the R^2 values for estimating the weight and volume of Thai apple berries were 0.955 and 0.965, respectively, while the MLR model provided R^2 values of 0.967 and 0.972 for weight and volume, respectively. All the above information revealed that CV based on a combination of image processing and traditional ML could estimate the weight and volume of fruit with high performance. This proposed technique might also be used for predicting the weight and volume of lime. Nevertheless, parameter optimization in the ML algorithm is necessary to generate a robust ML model. The learning process is regulated by a parameter called a hyperparameter, whose value must be adjusted to achieve optimal results [9]. Hyperparameters' adjustment of each machine learning algorithm needs to be internally performed and assessed based on the existing dataset. The values of hyperparameters can significantly impact the performance of a model; however, the selection of hyperparameters requires expertise and is time- as well as labor-intensive in the manual iterations. In practice, the automatic optimization of hyperparameters (AOH) is efficiently applied to ML models. Following the AOH procedure, the optimal architecture for an ML model is anticipated [10]. Therefore, the AOH is an important procedure for training ML models; however, when traditional ML techniques

are employed in computer vision, there are some limitations. Traditional ML methods can only deal with one-dimensional data, whereas the images are in a two-dimensional format. In contrast, digital images can be directly utilized as inputs for deep learning (DL).

Recent advances in the post-harvest process, the combination of CV and DL, have been adopted in the quantitative and qualitative evaluation of fruit and vegetable quality. DL is a subset of machine learning in which image data are used as inputs and the algorithm learns to recognize patterns within their spatial dimensions [11]. Convolutional neural networks (CNNs), which consist of numerous processing layers, are some of the most popular DL architectures for CV. CNNs can automatically recognize patterns in image data without using feature extraction techniques. In the long run, CNNs can simplify model construction and preprocessing, which reduces the complexity of the process and enhances the performance of the model. Previous studies have reported the utilization of CNNs for CV, especially in regression tasks for agricultural and food products, such as the estimation of Harumanis mango weight [12], the on-plant size and weight evaluation of tomato fruits [13], and the prediction of the firmness and sugar content of peach [14]. Ismail et al. (2020) developed a new CNN architecture (MangoMassNet) for estimating the mass of Harumanis mangoes from RGB images [12]. The results presented CNN architectures capable of predicting mango mass estimation with a mean squared error (MSE) value of 0.00227 and a mean average error (MAE) value of 0.03697. The size and weight of tomato fruits were studied by Hong et al. (2024) using deep neural networks and RGB-D imaging [13]. The prediction model estimated the tomato fruit weight with an RMSE of 19.69 g and a MAPE of 9.44%. The application of deep learning to RGB images of peaches for predicting firmness and sugar content was investigated by Masuda et al. (2023) [14]. The CNN regression models revealed the prediction results of skin color, flesh firmness, and sugar content with r = 0.91, 0.77, and 0.64, respectively. These studies showed the possibility of applying a CNN algorithm for the quantitative analysis of agricultural and food products; however, it is time-consuming to develop new CNNs for specific tasks, define the optimal architecture, and train the network. Transfer learning can solve these issues by training the pre-trained network and adjusting the input and output layers to learn a new dataset [15]. Several well-known pre-trained networks were developed for various analysis purposes, such as ResNet, VGG, Inception, and MobileNet. In addition, the pre-trained network can be employed when the size of the dataset is not suitable for training the model [15].

The literature review reveals that there is no report on the application of CV based on traditional ML and DL for estimating the weight and volume of lime fruit (*Citrus aurantifolia* (Christm.) Swingle). Therefore, this work focuses on developing a rapid essential protocol for evaluating lime weight and volume. Eight traditional ML algorithms, including PLS, ε-SVR, DT, RF, AB, GB, BME, and ERTs, were applied to train prediction models, and the optimal hyperparameters of each algorithm were automatically tuned to provide robust models. The geometric shape features (i.e., projected area, perimeter, major axis length, minor axis length, eccentricity, and radial distance) were extracted from images of limes to develop traditional ML models. In addition, four popular pre-trained DL architectures, including InceptionV3, MoblieNetV2, Resnet50, and VGG-16, were adapted for regression tasks and trained models for predicting the weight and volume of lime fruit. This study makes several key contributions to literature by introducing a novel approach that has not been widely explored in prior research. First, it also provides a comprehensive comparison between traditional ML algorithms and DL models, offering insights into the relative strengths of each approach in agricultural applications. Importantly, this research fills a gap in the literature by applying a diverse range of models, including tree-based (DT) and ensemble learning techniques (RF, AB, GB, BME, and ERTs), alongside deep learning methods. Furthermore, a significant contribution of this work lies in the automatic fine-tuning of hyperparameters in traditional ML algorithms, optimizing their performance in estimation tasks. This process enhances the accuracy and robustness of traditional models, making them competitive with deep learning architectures, thereby

offering practical solutions for agricultural applications that require fewer computational resources. Additionally, this study addresses limitations in traditional ML by incorporating advanced deep learning methods which allow for better feature extraction and pattern recognition. The findings highlight the potential for these methods to be integrated into automated agricultural systems for fruit sorting and grading, addressing key industry needs for scalability and efficiency. The scalable nature of the methodology makes it adaptable for other fruit types and broader agricultural settings, contributing to the advancement of digital agriculture and precision farming.

2. Materials and Methods

2.1. Sample Collection of Limes

The experiment was carried out in August 2023, which is the main harvest season for limes in Thailand. A total of 126 fresh limes of various sizes were gathered from a local market in Bangkok, Thailand. The lime samples were normal shapes and free from any visible injuries and defects. Before the experiment, the fruit samples were cleansed with distilled water, drained, and then wiped with paper towels to remove excess water from their surfaces. The samples were kept at room temperature (25 °C) until image acquisition.

2.2. Image Acquisition of Limes

Each image of limes was captured in a photo box studio (with a length, width, and height of about 45 cm, 45 cm, and 45 cm, respectively) with LED lighting. Dual light-emitting diode (LED) strips were installed in the photo box studio, and the light-emitting capability of each lump strip was 10 W. The camera and lens used were a Basler ACA2500-14UC and Basler C125-0818-5M F-1.8, F-8mm (Basler AG, Ahrensburg, Germany) respectively. A white surface was used on the bottom surface of the photo box studio to generate a uniform background. Figure 1 presents a schematic diagram of the image acquisition system for limes, and Table 1 provides a summary of this image sensor's characteristics. The tuning capture type uses continuous capture with a sample distance with a camera of about 150 mm, using Pylon Viewer 7.2.0.11624 software. Each lime was acquired at four different orientations images, including the top, left, right, and bottom sides of the fruit. During the image acquisition period, all 126 lime samples were subjected to an identical procedure. Therefore, the total number of images was 504 images.

Table 1. Specifications of the camera and lens used in this study.

Basler ACA2500-14UC	Sensor type	CMOS
	Sensor size	5.7′4.3 mm
	Resolution (H′V)	2590′1942 px
	Resolution	5 MP
	Pixel size (H′V)	2.2′2.2 µm
	Frame rate	14 fps
	Pixel bit depth	12 bits
	Housing size (L′W′ H)	29.3′29′29 mm
	Operating Temperature	0–50 °C
	Weight	80 g
Basler Lens C125-0818-5M-P f8mm	Focal length	8.0 mm
	Lens mount	C-mount
	Iris	F1.8–F22.0
	Iris type	Manual
	IR cut filter	No
	Pixel pitch	2.20 µm
	Sensor format	1/2.5″
	Min. working distance	100 mm

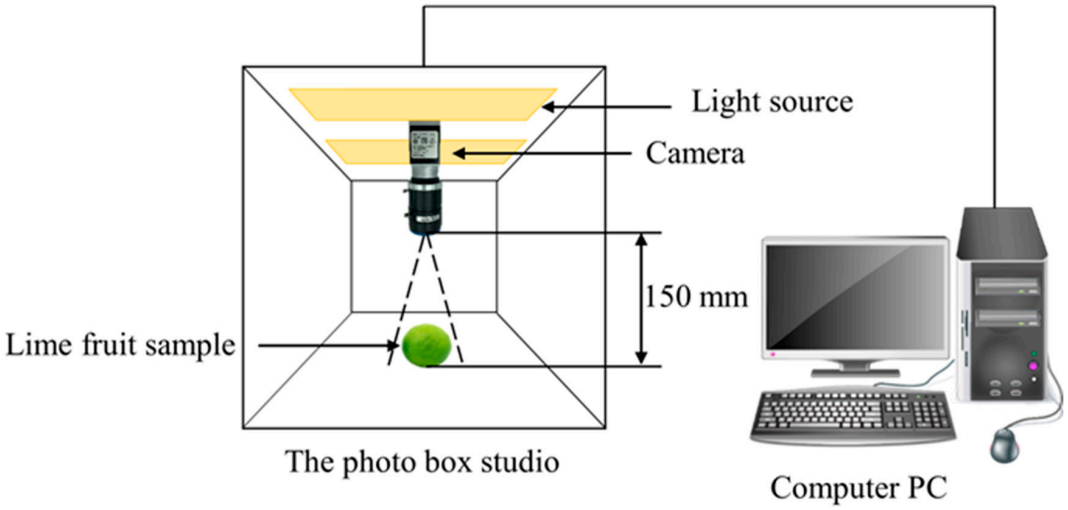

Figure 1. Schematic diagram of the lime image acquisition system.

2.3. Measurement of the Weight and Volume of Limes

The lime samples were weighed using an electronic balance (ML104T/00 model, Mettler-Toledo Ltd., Melbourne, Australia) with an accuracy of ±0.1 mg. After weighing, the volume of fruit was determined by WDM, which is one of the most common and straightforward methods for measuring the volumes of fruits and vegetables [4,16]. The volume of fruit was calculated using the following equation [4,16]:

$$\text{Volume } (\text{cm}^3) = \frac{\text{weight of displaced water } (\text{g})}{\text{water density } (\frac{\text{g}}{\text{cm}^3})} \quad (1)$$

where water density is 1000 g/cm^3. Though it is highly accurate, this methodology may be deemed intrusive or damaging for certain products, and it is not recommended for objects that absorb water [3].

2.4. Development of Traditional Machine Learning Models

2.4.1. Image Processing and Feature Extraction

Image processing and feature extraction were conducted using Python (version 3.9.7, Python Software Foundation, Wilmington, DE, USA) with the OpenCV (version 4.6.0.66) package for computer vision. The raw images were pre-processed before feature extraction, with the following procedure: (1) grayscale image conversion, (2) background removal using Otsu's method [17] with binarization, and (3) the detection of the contour of a lime's shape. Figure 2 presents raw image, grayscale image, binary image, and contour line image of lime. After pre-processing, the geometric shape features, including the projected area, perimeter, major axis length, minor axis length, eccentricity, and radial distance, were extracted from each image of lime. These features were used to develop traditional ML.

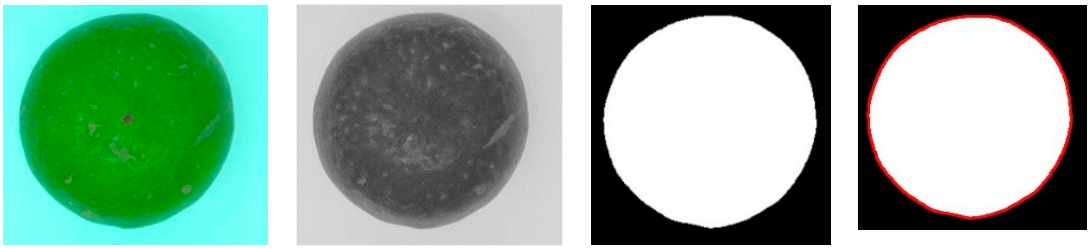

(**a**) (**b**) (**c**) (**d**)

Figure 2. Lime image: with raw image (**a**), grayscale image (**b**), binary image (**c**), and contour line image (**d**).

2.4.2. Statistical Analysis

The maximum (Max), minimum (Min), mean, and standard deviation (SD) of the weight and volume were calculated. The Pearson's correlation coefficients (r) among features from image, weight, and volume were calculated with a confidence level of 95%. Principal component analysis (PCA) was performed on the data of weight, volume, and the six features from lime images. The score plot was created from the first two principal components (PCs) for understanding the data's underlying patterns and outliers. The 95% confidence ellipse is based on Hotelling T^2 statistics. In addition, outliers were detected by the plots of residuals and leverages. The residuals define the degree to which samples or variables fit PCA, as determined by PCs. The samples with high residuals are poorly represented by PCA, although they are well described by other samples. These samples are strangers to the well-described samples, i.e., outliers. The leverages define the distance from the projected sample (i.e., its PCA approximation) to the center (mean point). The samples with high leverage have a stronger influence on the model than other samples; they may or may not be outliers, but they are influential. An influential outlier (high residual + high leverage) is the worst case; it can, however, easily be detected by using an influence plot. A sample with high residual was specified to be an outlier.

2.4.3. Machine Learning Modeling

Estimation models for weight and volume were developed using partial least square regression (PLS), epsilon-support vector regression (ε-SVR), decision tree (DT), random forest (RF), adaptive boosting (AB), gradient boosting (GB), Bagging meta-estimator (BME), and extremely randomized trees (ERTs). Six geometric shape features were used to train the ML estimators. The dataset was randomly split into 2 groups, including the training set (80% of all samples) and the testing set (20% of all samples). Therefore, the number of images in the training set and the testing set was 404 and 100 images, respectively. The splitting train and test set was performed using the train_test_split function of the Scikit-learn package with the number of random_state of 100. The modeling process was carried out in Python (version 3.9.7, Python Software Foundation, Wilmington, DE, USA) using Scikit-learn ML packages (Version 1.1.3) and the Jupyter Notebook programming tool (Version 6.5.2). The training set was adopted to fine-tune the optimum hyperparameter of each ML algorithm with the GridSearchCV command of the Scikit-learn module. Figure 3 presents the algorithmic flow diagram of the proposed traditional ML system. The predefined parameter for searching for the optimum hyperparameter is shown in Table 2. According to the lowest root mean square error of cross-validation (RMSECV), the best hyperparameter was revealed by performing 10-fold cross-validation. The coefficient of determination of the training and testing sets (R^2_{train} and R^2_{test}), the root mean square error of the training and testing sets ($RMSE_{train}$ and $RMSE_{test}$), the mean absolute percentage error of the training and testing sets ($MAPE_{train}$ and $MAPE_{test}$), and the ratio of prediction to deviation (RPD) were used for the assessment of model performance.

Table 2. Predefined parameter for performing the GridSearchCV command on 10-fold cross-validation.

Algorithm	Hyper-Parameter	Turning Range
PLS	n_components	1–20
ε-SVR	kernel	linear, poly, rbf, sigmoid
	C	100–1000
	degree	2–5
	gamma	0.001–0.09
	coef0	0.001–0.09
DT	min_samples_leaf	1–10
	min_samples_split	2–20

Table 2. *Cont.*

Algorithm	Hyper-Parameter	Turning Range
RF	n_estimators max_depth	100–1000 2–11
AB	n_estimators learning_rate	20–500 0–0.2
BME	n_estimators max_samples max_features	20–100 1–100 1–20
ERT	n_estimators min_samples_leaf min_samples_split	20–100 1–10 2–20
GB	n_estimators learning_rate min_samples_leaf min_samples_split	20–100 0–0.2 1–10 2–20

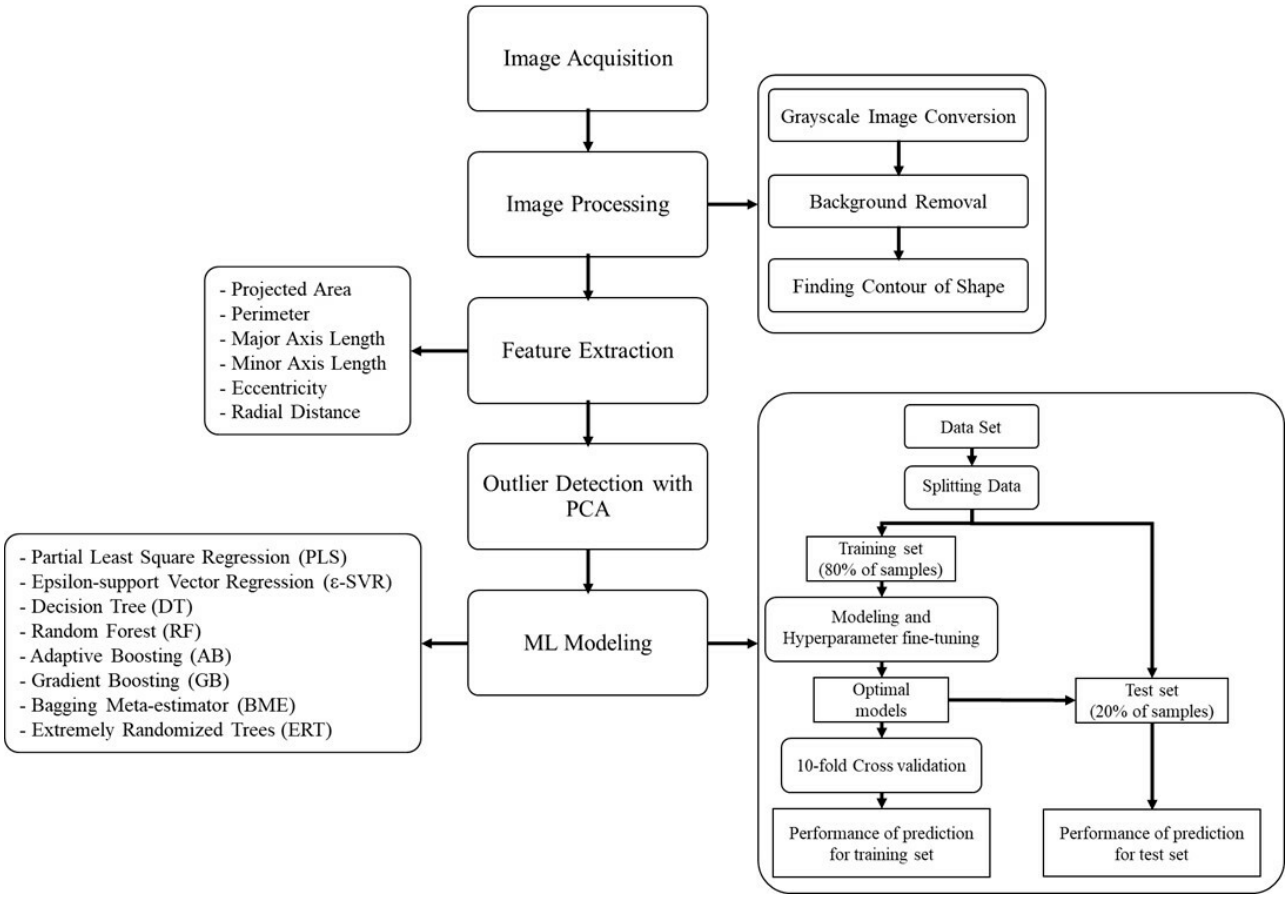

Figure 3. The algorithmic flow diagram of the proposed traditional ML system.

2.5. Development of Deep Learning Models

Generally, CNNs' learning procedures need sufficient training image sets to develop high-performance models. Due to overfitting, an insufficient dataset produces inaccurate outcomes which are difficult to apply in practice [18]. Data augmentation is a popular approach to overcoming the limitations of image datasets [19]. In this study, three image augmentation techniques, including flipping, rotation, and brightness enhancement, were randomly applied 10 times to each lime sample image. Flipping was performed on an

image around its vertical axis, horizontal axis, or both the vertical and horizontal axes. The rotation process was carried out in the right direction or the left direction via the randomization of angles between −45 and 45 on an image around an axis. The brightness adjustment was applied with a randomization of the brightness factor between 0.5 and 1.5. The number of images after the image augmentation process was 5040 pieces of data. All image data were resized into 128 × 128 pixels, and a normalization procedure was then applied to scale pixel values to a standard range between 0 and 1. The dataset of images was defined for the training set and testing set with a ratio of 80:20 (using 4032 and 1008 samples, respectively) with the same procedure in Section 2.4.3. The raw and augmented images are shown in Figure 4.

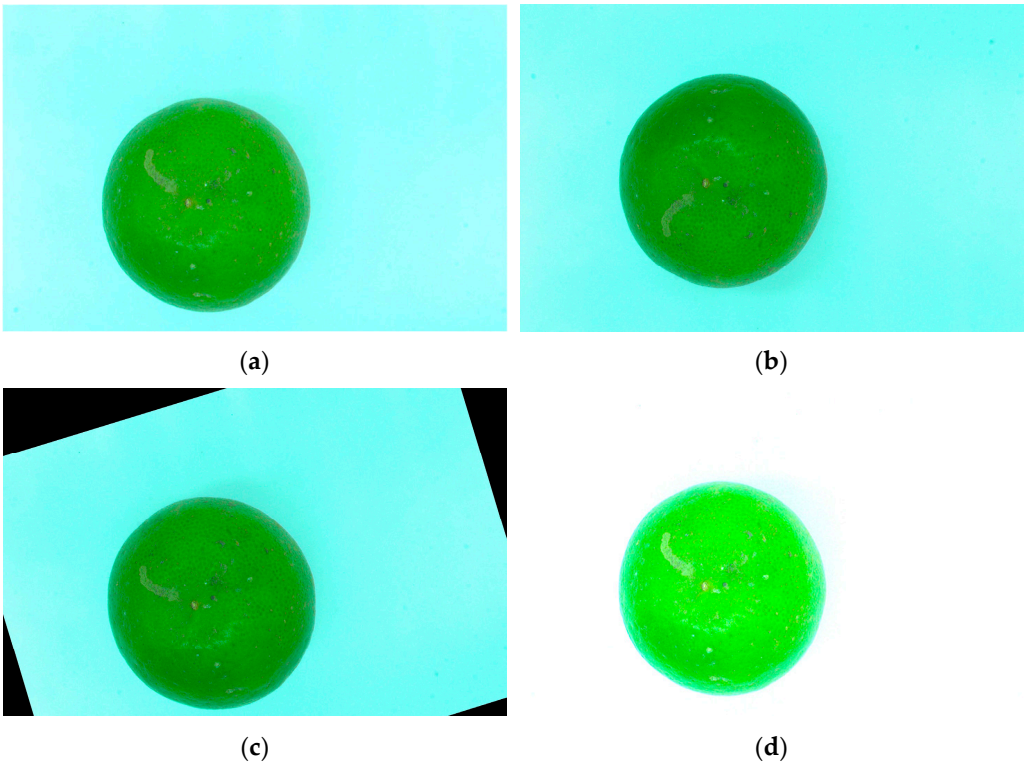

Figure 4. Raw image (**a**) and augmented images with flipping (**b**), rotation (**c**), and brightness adjustment (**d**).

For DL training, the four proposed pre-trained structures for estimating the weight and volume of limes were applied, including InceptionV3, MobileNetV2, ResNet50, and VGG-16. Each pre-trained model was connected to two dense layers activated by the rectified linear unit (ReLU) function. The final output layer employed the linear activation function for the regression task. Model optimization was performed using the Adam optimizer. The batch size, epochs per running, and validation split were 32, 100, and 10%, respectively. The MSE against epochs from training all pre-trained DL architectures was plotted to assess the training speed. The R^2_{train}, R^2_{test}, $RMSE_{train}$, $RMSE_{test}$, $MAPE_{train}$, $MAPE_{test}$, and RPD were used for the assessment of model performance. In this study, Google Colab Pro was utilized with an NVIDIA A100 Tensor Core GPU. The DL process in this project was carried out with an open-source library (TensorFlow Version 2.17.0). The algorithmic flow diagram of the proposed DL system is presented in Figure 5.

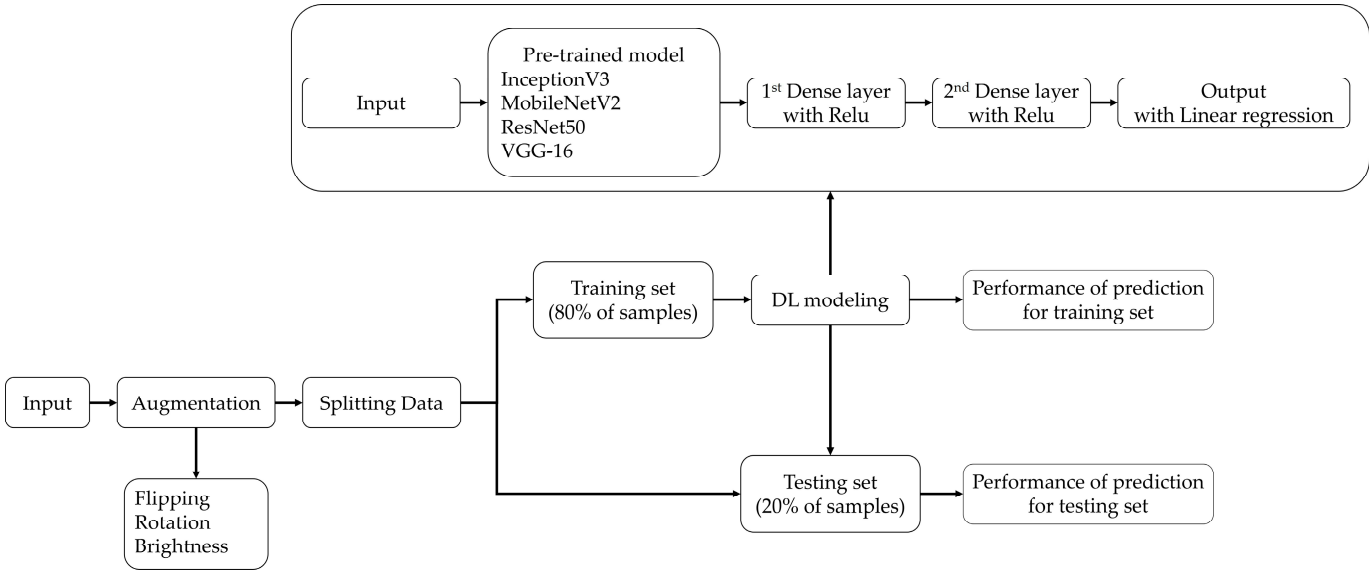

Figure 5. The algorithmic flow diagram of the proposed DL system.

3. Results and Discussions

3.1. Descriptive Statistic of Dataset

The statistical data of the weight and volume of fresh limes are shown in Table 3. The weight ranges of limes for the training and testing sets are about 23.80 to 46.02 g and 24.44 to 46.02 g, respectively. For the volume, the range of the training set was 20 to 45 cm^3, and that of the testing set was 24 to 45 cm^3. The range of the training set of weights was narrower compared to the volume. The range and standard deviations of the dataset have an impact on the performance of the ML model. The inefficiency model was caused by the extremely narrow ranges of the target variable and very low standard deviations, while a wide range and high standard deviations lead to a more efficient model [20]. Specifically, a large dataset representing wide variability (fruit size, variety, and harvest time) could increase the range and standard deviations of the dataset.

Table 3. The statistical data of the weight and volume of fresh lime.

Property of Lime	Training Set				Testing Set			
	Minimum	Maximum	Mean	SD	Minimum	Maximum	Mean	SD
Weight (g)	23.80	46.02	36.43	5.53	24.44	46.02	38.87	5.66
Volume (cm^3)	20.00	45.00	35.68	5.77	24.00	45.00	36.43	5.77

3.2. Correlation Among Feature, Weight, and Volume

In this research, the relationship between variables is examined with the Pearson correlation method. The Pearson correlation method is the most common method to use for numerical variables when studying the relationship between two variables. Pearson's correlation matrix is presented in Table 4, showing the relationships between various lime features, weight, and volume. Among all measured features, the major axis length exhibits the strongest positive correlation with weight (r = 0.835). Similarly, the major axis length also displays a robust positive association with volume (r = 0.867). This suggests that major axis length is the most important feature of lime images. Furthermore, the area feature seems to be the second most important feature after the major axis length, with positive correlation coefficients of 0.817 for weight and 0.845 for volume. The Pearson correlation method assigns a value of r between −1 and 1, where 0 indicates no correlation, 1 indicates a total positive correlation, and −1 indicates a total negative correlation [21]. Most of the features are area, perimeter, major axis length, and minor axis length. These

features are related to the weight and volume of lime, with r values greater than 0.718. A correlation value of more than 0.718 for two variables indicates that a significant and positive relationship exists between them. A positive correlation signifies that if the variable features increase, then the weight and volume will also increase. Therefore, it is possible to evaluate the weight and volume of lime from an image based on the above relationship; however, the features of eccentricity and radial distance had a less pronounced effect on the weight and volume of lime.

Table 4. A Pearson's correlation matrix of the features, weight, and volume of lime.

	Weight	Volume	Area	Perimeter	Major Axis Length	Minor Axis Length	Eccentricity	Radial Distance
Weight	1							
Volume	0.772	1						
Area	0.817	0.845	1					
Perimeter	0.798	0.826	0.950	1				
Major Axis Length	0.835	0.867	0.914	0.903	1			
Minor Axis Length	0.718	0.744	0.957	0.890	0.761	1		
Eccentricity	−0.099	−0.103	−0.367	−0.278	0.036	−0.619	1	
Radial Distance	0.048	0.057	0.039	0.033	0.048	0.029	0.013	1

3.3. Principal Component Analysis

In Figure 6a, the score plot between PC1 and PC2 was used to show the relationship variables in a dataset, with the PC1 axis showing the direction with the highest variance (100%) in the data. The PC2 axis shows the direction with the lowest variance (0%). The circled green points distributed outside of the blue triangle were considered outliers of lime samples with 95% confidence based on Hotelling T^2. For Figure 6b, the plot between the residual and leverage was observed as the outliers on top of the plot, which has a high value for the residual (circle red points). This can be noticed in the downward pull of the model. The outliers with a high residual were removed. In this research, outliers can be caused by incorrect measurements or the incorrect recording of weight and volume. Therefore, all outliners were removed before the development of the model to improve the precision in estimation. The number of remaining samples was about 466.

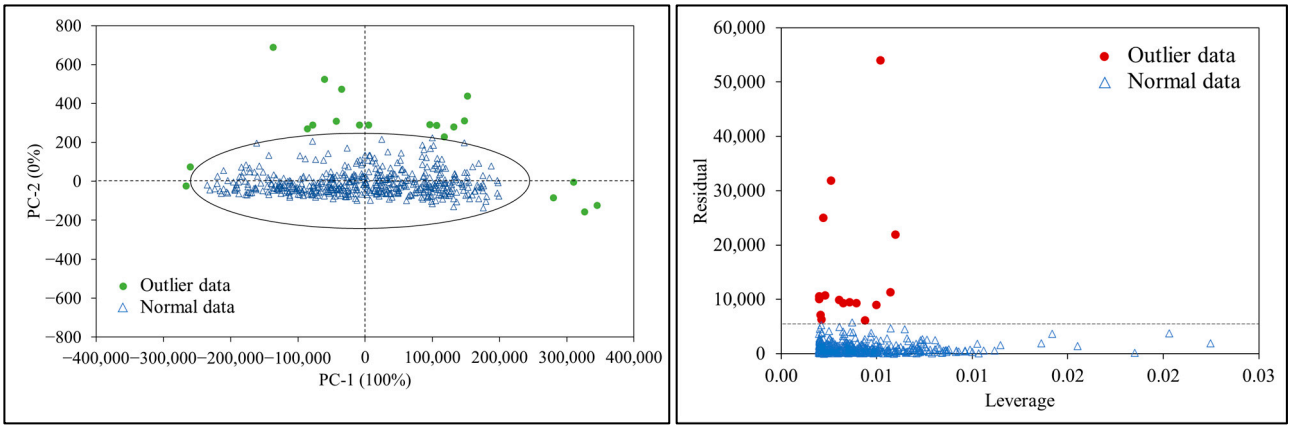

(**a**) (**b**)

Figure 6. Outlier removal using PCA plot. (**a**) PC1 vs. PC2 of PCA. (**b**) Residual vs. leverage plot.

3.4. Performance of Traditional Machine Learning Algorithms

The optimal hyperparameters for weight and volume are obtained from the following algorithms: PLS, ε-SVR, DT, RF, AB, BME, ERT, and GB. These algorithms were used to evaluate the weight and volume of limes. The details of the configuration of the hyperparameters are shown in Table 5. The choice of algorithms and hyperparameters for developing computer vision models using traditional ML approaches depends on an analysis of dataset characteristics. This study chose the optimal algorithm and hyperparameters to develop the best calibration models.

Table 5. The optimal hyperparameters for weight and volume.

Algorithm	Optimal Hyperparameter	
	Weight	**Volume**
PLS	n_components = 6	n_components = 5
ε-SVR	degree = 2 kernel = 'poly'	degree = 2 kernel = 'poly'
DT	ccp_alpha = 0.1 max_features = 5 min_impurity_decrease = 0.1 min_samples_leaf = 0.1 min_samples_split = 0.1	ccp_alpha = 0.2 max_features = 4 min_impurity_decrease = 0.1 min_samples_leaf = 0.1 min_samples_split = 0.1
RF	ccp_alpha = 0.4 max_features = 4 min_impurity_decrease = 0.2 min_samples_leaf = 0.1 min_samples_split = 0.2 n_estimators = 110	ccp_alpha = 0.1 max_features = 5 min_impurity_decrease = 0.1 min_samples_leaf = 0.1 min_samples_split = 0.2 n_estimators = 30
AB	learning_rate = 0.32 n_estimators = 120	learning_rate = 0.04 n_estimators = 90
BME	max_features = 4 max_samples = 160 n_estimators = 80	max_features = 5 max_samples = 110 n_estimators = 130
ERTs	max_features = 6 min_samples_leaf = 0.1 min_samples_split = 0.1 n_estimators = 140	max_features = 6 min_samples_leaf = 0.1 min_samples_split = 0.2 n_estimators = 60
GB	max_features = 2 min_samples_leaf = 0.1 min_samples_split = 0.1 n_estimators = 60	max_features = 2 min_samples_leaf = 0.1 min_samples_split = 0.2 n_estimators = 110

The results of different traditional ML algorithms for predicting the weight and volume of limes are represented in Table 6. The results showed that all models had good performance values (i.e., R^2_{train}, R^2_{test}, $RMSE_{train}$, $RMSE_{test}$, $MAPE_{train}$, $MAPE_{test}$, and RPD) with slightly different performances. For weight prediction, the best model, the BME model, achieved the following performance metrics: the highest R^2 for both training and testing (0.983 and 0.954), the lowest $RMSE_{train}$, $RMSE_{test}$, $MAPE_{train}$, and $MAPE_{test}$ (0.723, 1.205, 1.526, and 2.530, respectively), and the highest RPD (4.697). A model R^2 value in the range of 0.92–0.96 is usable in most applications, including quality assurance [22]. For volume prediction, the best model achieved the following performance metrics: the highest R^2 for both training and testing (0.907 and 0.882), the lowest $RMSE_{train}$, $RMSE_{test}$, $MAPE_{train}$, and $MAPE_{test}$ (1.760, 1.971, 3.842, and 4.151, respectively), and the highest RPD (2.927) (the BME model). A model with an R^2 range from 0.83 to 0.90 is usable with caution for most applications, including research [22]. A high RPD indicates efficient prediction because the

standard error of prediction should be lower than the standard deviation. Figures 7 and 8 illustrate the relationship between the estimated and real values of weight and volume of the PLS, ε-SVR, DT, RF, AB, BME, ERTs, and GB algorithms. Scatter plots of the estimated values versus the real weight and volume are present in Figures 7 and 8, respectively. This research proposes novel models for predicting the weight and volume of limes with high accuracy. These models can be valuable tools for future research and applications. The shape of the lime was found to be an important factor in predicting its weight and volume. Several studies have investigated ML algorithms for predicting the weight and volume of various fruits using computer vision techniques. An applied LR model combined with image processing techniques to predict strawberry weight was proposed. That model achieved a maximum R^2 of 96.3% and 89.6 for the training and testing stages, respectively, in predicting the relationship between pixel numbers and fruit weight [23]. Research on the volume estimation of strawberries using a combination of image processing techniques and LR is reported, and the result shows that the high correlation between estimated and actual volumes was the most suitable, with an R^2 of 0.866 [24]. A study on estimating the weight parameters of selected wheat refractions using image processing is proposed. The result shows a linear relationship between the volume of refractions derived from measured dimensions and calculated from images, with R^2 values ranging from 0.845 to 0.945 [25]. Calixto et al. (2019) [6] reported a LR model capable of predicting the weight of yellow melon by using the area of fruit as an independent variable with a Pearson's correlation of 0.989. While strong predictive performance was revealed with high Pearson's correlation in these previous studies, the use of a simple linear model may limit the model's flexibility when applied to more complex datasets or fruits with irregular shapes. In addition, LR might not fully capture the complex, non-linear relationships between a fruit's area and its weight. In our study, the use of multiple features, such as projected area, perimeter, major axis length, minor axis length, eccentricity, and radial distance, provides a more comprehensive representation of the fruit's geometry compared to the single-area feature used in their studies. This richer set of features allows our ML models to capture more complex relationships between a fruit's shape and its weight and volume, leading to potentially higher prediction accuracy and better generalization across different fruit samples. By incorporating these additional geometric properties, our models are less likely to be affected by the limitations of using a single feature, offering more robustness and precision in real-world applications. The use of multiple geometric properties in ML modeling has been studied by Nyalala et al. (2021), Nyalala et al. (2019), and Mansuri et al. (2022) [5,7,8]. These studies achieved high accuracy in the estimation of the weight and volume of fruit by using MLR, SVR, and ANNs. In contrast, our research utilized a more diverse range of models, incorporating traditional ML algorithms, such as DT, and ensemble learning methods, like RF, AB, GB, BME, and ERTs. This broader range of models allowed for a more comprehensive analysis and comparison of techniques, leading to improved model performance and robustness. By exploring diverse traditional ML methods, our research offers a more versatile solution for predicting weight and volume, achieving high accuracy across different algorithms while ensuring flexibility and adaptability in practical applications. A potato grading system of weight and shape using image processing that uses the PCA algorithm is proposed. The accuracy of classification was 90%, 100%, and 90% for large, medium, and small sizes, respectively [26]. Our study extends beyond simple classification by utilizing various ML models for precise continuous predictions of weight and volume in lime fruit. This distinction highlights a key difference: while the potato grading system uses dimensionality reduction for discrete classification, our approach employs comprehensive models for regression tasks, predicting exact values, which could be adapted for a broader range of applications in various fruits.

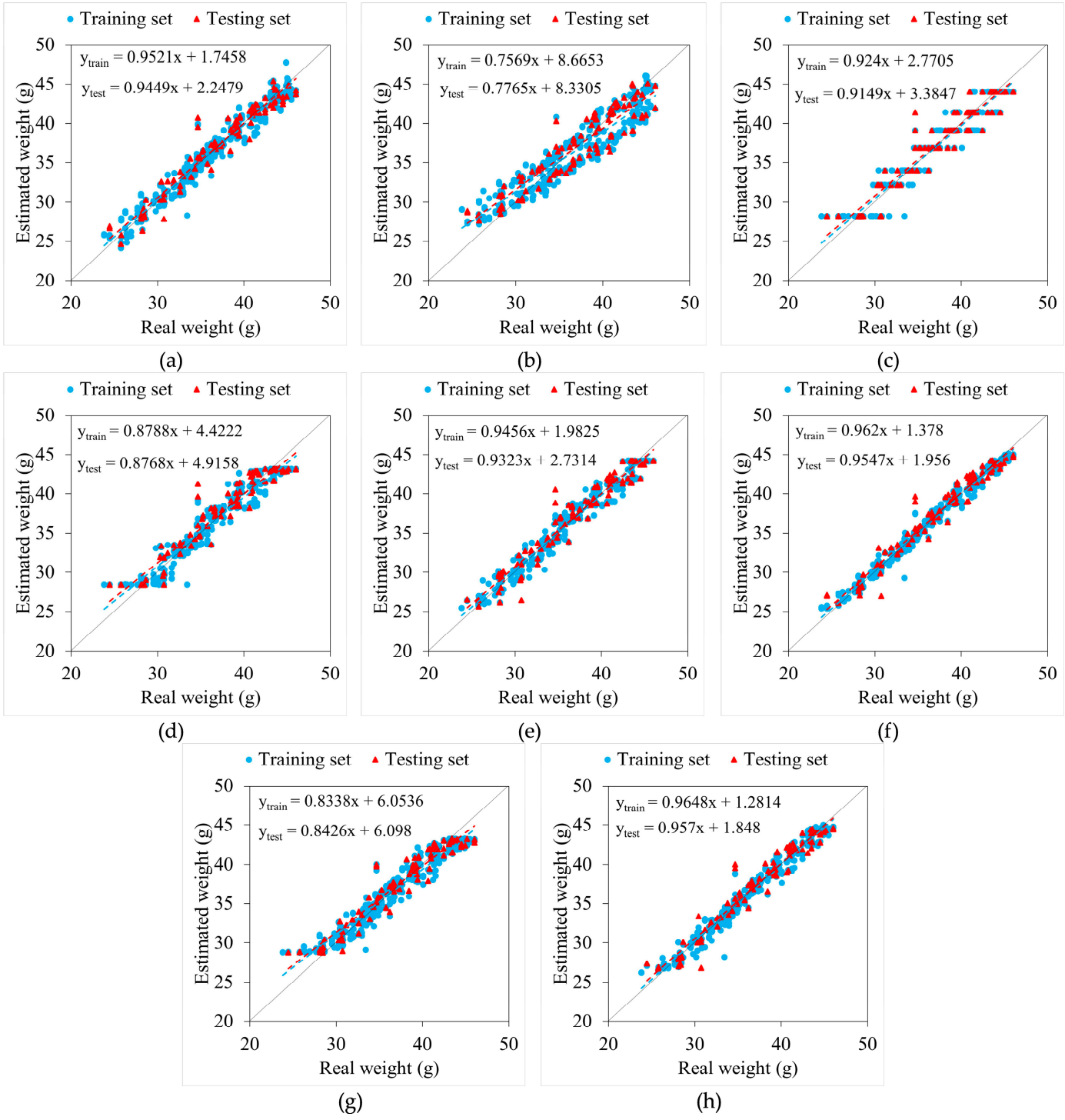

Figure 7. Scatter plots of the estimated and real weights for each algorithm: (**a**) PLS, (**b**) ε-SVR, (**c**) DT, (**d**) RF, (**e**) AB, (**f**) BME, (**g**) ERTs, and (**h**) GB.

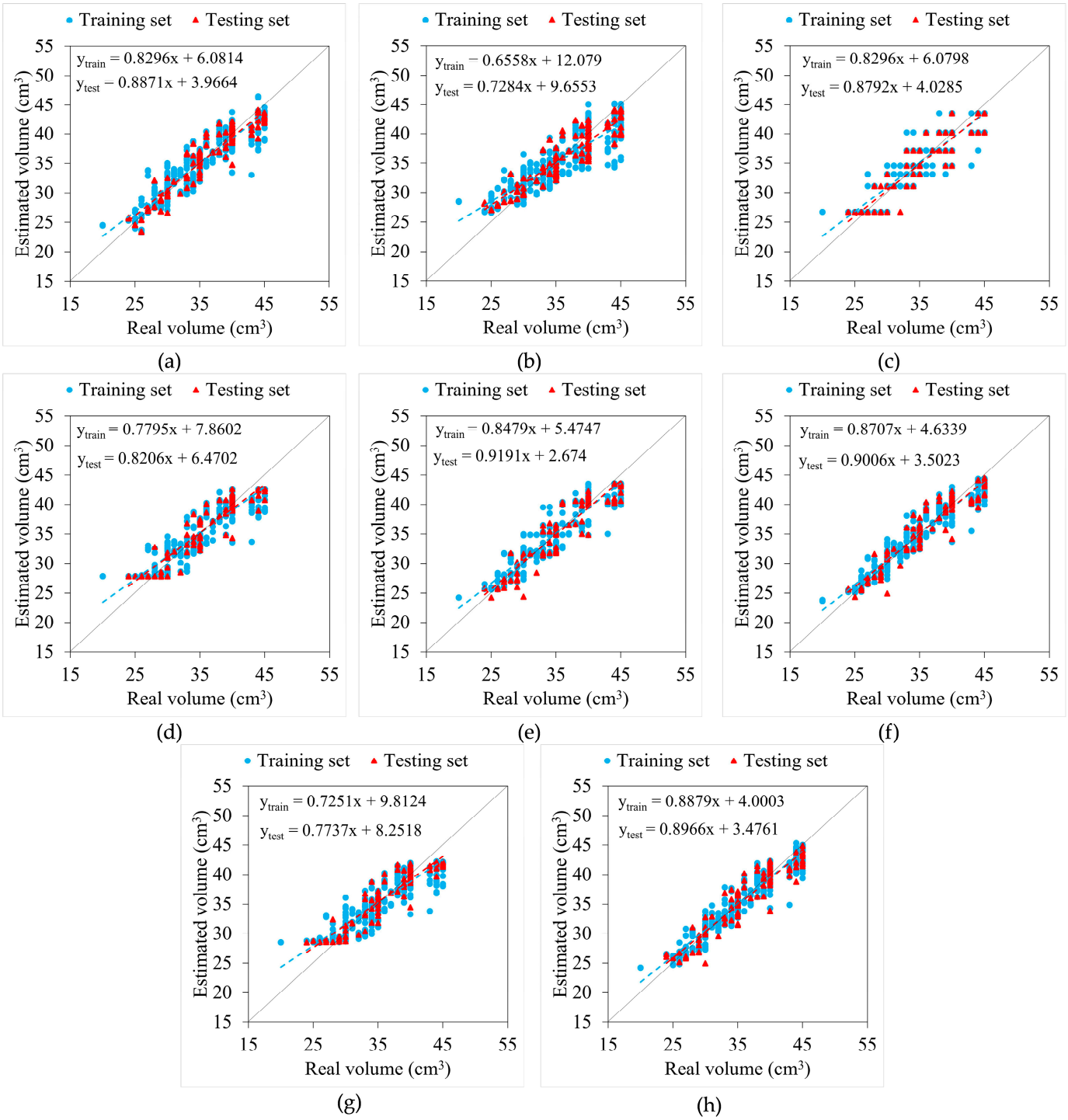

Figure 8. Scatter plots of the estimated and real volumes for each algorithm: (**a**) PLS, (**b**) SVM, (**c**) DT, (**d**) RF, (**e**) AB, (**f**) BME, (**g**) ERTs, and (**h**) GB.

Table 6. Prediction results of the determination of the weight and volume of fresh limes via traditional machine learning.

	Algorithm	R^2_{train}	R^2_{test}	$RMSE_{train}$	$RMSE_{test}$	$MAPE_{train}$ (%)	$MAPE_{test}$ (%)	RPD
Weight (g)	PLS	0.952	0.940	1.210	1.400	2.604	2.866	4.043
	ε-SVR	0.850	0.855	2.160	2.144	5.087	4.919	2.640
	DT	0.924	0.910	1.524	1.690	3.356	3.385	3.349
	RF	0.935	0.914	1.413	1.651	3.098	3.429	3.428
	AB	0.959	0.933	1.117	1.463	2.551	3.215	3.869
	BME	0.983	0.954	0.723	1.205	1.526	2.530	4.697
	ERT	0.927	0.917	1.489	1.625	3.376	3.482	3.483
	GB	0.972	0.942	0.922	1.356	1.916	2.721	4.174
Volume (cm^3)	PLS	0.830	0.880	2.380	1.981	5.432	4.333	2.857
	ε-SVR	0.724	0.810	3.026	2.500	6.855	5.572	2.308
	DT	0.830	0.845	2.380	2.260	5.373	5.023	2.553
	RF	0.824	0.858	2.423	2.159	5.691	4.936	2.673
	AB	0.860	0.867	2.155	2.090	4.866	4.609	2.761
	BME	0.907	0.882	1.760	1.971	3.842	4.151	2.927
	ERT	0.800	0.850	2.596	2.225	6.108	4.989	2.593
	GB	0.892	0.880	1.892	1.986	3.690	4.614	2.905

To identify the most important features influencing the weight and volume of limes, PLS was used to calculate regression coefficients. The principle of the regression coefficients could be investigated to explore the relationship between predictor variables and responses [27]. The regression coefficient values from PLS for predicting the weight and volume of limes are presented in Table 7. The major axis length was the highest regression coefficient among area, perimeter, minor axis length, eccentricity, and radial distance in terms of both weight and volume. It showed that the major axis length feature estimates may significantly impact the model's performance in predicting the weight and volume of limes. The strong correlation between the major axis length and both the weight and volume of limes, as shown by Pearson's correlation matrix, supports these findings. This aligns with reports that fruit and vegetable volume is strongly related to shape, as demonstrated in studies on cabbage [28], peach [29], and peppers [30]. Additionally, the regression coefficient for the weight of the minor axis length is the second highest after that of the major axis. This finding suggests that both the major and minor axes play crucial roles in predicting the weight of limes; however, the analysis revealed that in cases where the regression coefficient for volume was the second most important area feature after the major axis length, suggesting that the major axis length and area of limes are the two most significant features for volume prediction. Hence, the result of this study indicated that these computer vision and machine learning algorithms can predict the volume and weight of limes from geometric and shape features in a non-destructive manner.

Table 7. The regression coefficient of the weight and volume of lime.

Geometric and Shape Features	Regression Coefficient	
	Weight	Volume
Area	3.073258	−1.162733
Perimeter	1.332884	0.409460
Major axis length	5.077340	5.978942
Minor axis length	−4.852905	−0.013067
Eccentricity	−2.330182	−0.992423
Radial distance	0.054030	0.214718

3.5. Performance of Deep Learning

The MSE against epochs of four pre-trained models (i.e., InceptionV3, MoblieNetV2, ResNet50, and VGG-16) for estimating weight and volume are shown in Figures 9 and 10, respectively. Because every model was trained from the beginning, its MSE for both training and validation began at a significantly higher value, and then subsequently decreased to a lower value, and then rather stabilized for the remaining epochs. The training speed of a DL model is an important evaluation characteristic of a loss function. A good loss function leads to a DNN with a lower estimation error for a fixed number of epochs [31]. The MSE for both the training and validation sets of the eight DL prediction models for the weight and volume decreased rapidly during the first 10 epochs which can indicate that all models are quickly learning to minimize errors; however, the validation error fluctuates throughout the training process, especially for the MoblieNetV2 model, for estimating weight. This erratic behavior could stem from the fact that the four pre-trained architectures are primarily designed for image classification tasks. While they can be adapted for regression, the unstable pattern observed in the validation error graph may arise from the continuous nature of the predicted values, where slight fluctuations in the input data lead to disproportionate variations in the model's predictions, resulting in instability during training. Therefore, careful modification of the output layer and loss function is necessary to ensure proper performance in predicting continuous values. If this adaptation is fine-tuned, it could lead to stability in learning, causing the model to be consistent between regions of the loss function. This point is an interesting issue for future study.

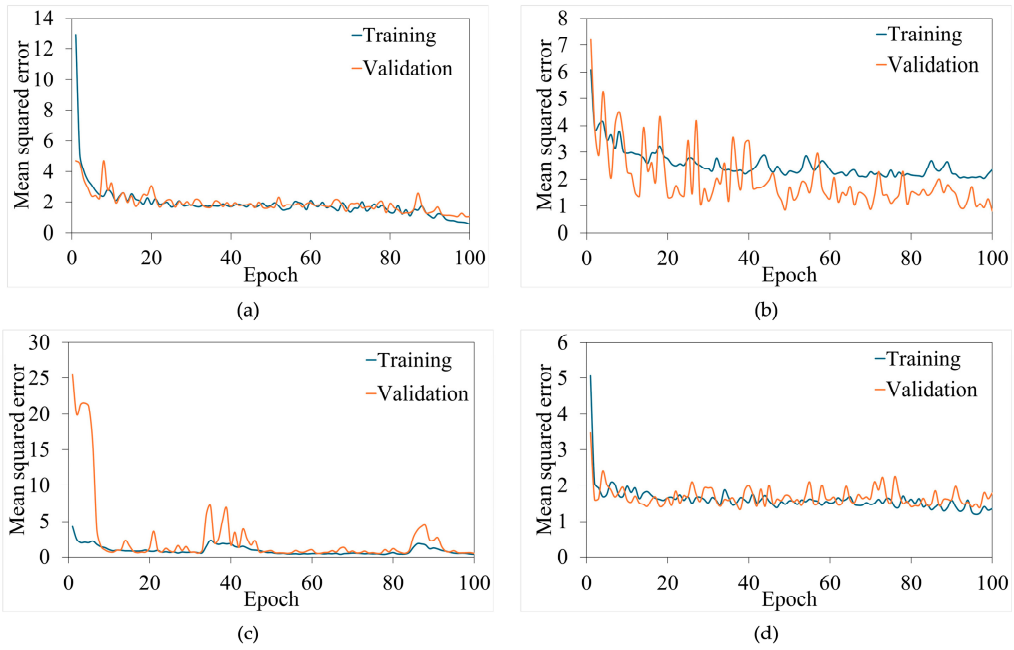

Figure 9. The mean square error against epochs of the InceptionV3 (**a**), MobileNetV2 (**b**), ResNet50 (**c**), and VGG-16 (**d**) models for estimating weight.

The results of four pre-trained models predicting the weight and volume of limes are represented in Table 8. All models presented high performance values (i.e., R^2_{train}, R^2_{test}, $RMSE_{train}$, $RMSE_{test}$, and RPD). The ResNet50 model produced the best weight prediction performance metrics: the highest R^2 for both training and testing (0.998 and 0.951), the lowest RMSE for training and testing (0.292 and 1.455), and the highest RPD (4.510). For volume prediction, the ResNet50 model also provides the best prediction with the highest R^2 for both training and testing (0.998 and 0.957), the lowest RMSE for training and testing (0.284 and 1.259), and the highest RPD (4.747). Williams et al. (2019) suggested that a model with a high R^2 (between 0.83 and 0.90) is usable with caution for most applications [22]. These points

indicate that the ResNet50 model can estimate the weight and volume of limes with high accuracy. In other words, this study may organize the performance of regressor analysis order according to its R^2 as MoblieNetV2 < VGG-16 < InceptionV3 < ResNet50 for weight and VGG-16 < InceptionV3 < MoblieNetV2 < ResNet50 for volume. Figures 11 and 12 demonstrate the relationship between the estimated values and real values for weight and volume of the InceptionV3, MoblieNetV2, ResNet50, and VGG-16 models. Ismail et al. (2020) [12] developed a custom CNN architecture (MangoMassNet) specifically designed to estimate the mass of Harumanis mangoes from RGB images, achieving a MSE value of 0.00227 and a MAE value of 0.03697. In contrast, our research utilizes established DL architectures, including InceptionV3, MobileNetV2, ResNet50, and VGG-16, which have been pre-trained on large datasets and are known for their robust feature extraction capabilities. While Ismail et al. focused on a tailored CNN model for a specific fruit, our approach leverages multiple proven architectures, allowing for a more comprehensive evaluation of performance and potentially improving the accuracy and generalizability of weight and volume estimations. These findings could serve as a valuable framework for applying similar techniques to estimate the weight and volume of other fruits.

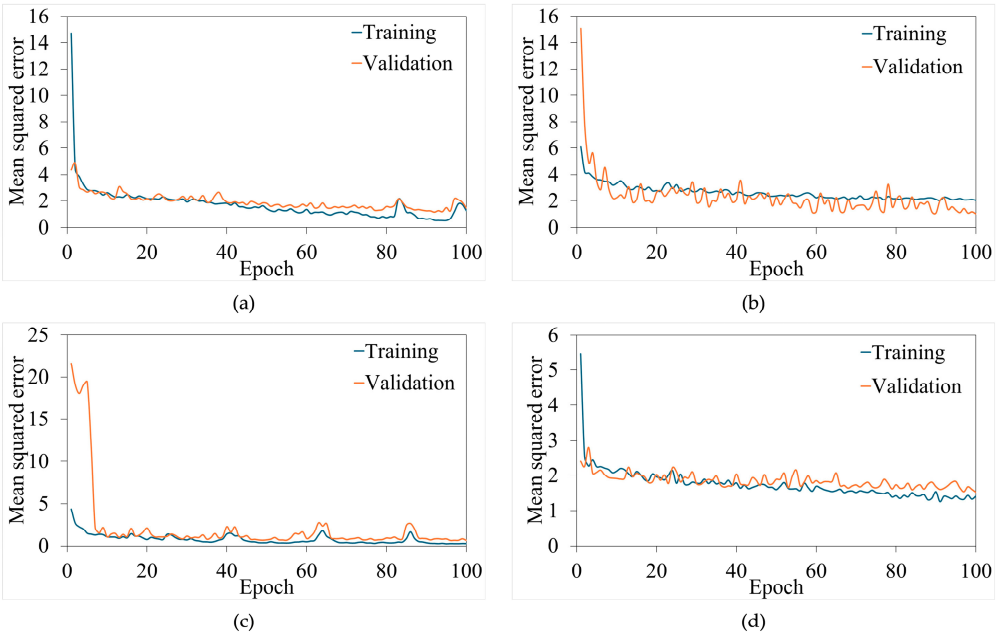

Figure 10. The mean square error against epochs of the InceptionV3 (**a**), MobileNetV2 (**b**), ResNet50 (**c**), and VGG-16 (**d**) models for estimating volume.

Table 8. Prediction results of the determination of the weight and volume of fresh limes via deep learning.

	Pre-Trained Model	R^2_{train}	R^2_{test}	$RMSE_{train}$	$RMSE_{test}$	$MAPE_{train}$ (%)	$MAPE_{test}$ (%)	RPD
Weight (g)	InceptionV3	0.983	0.853	0.878	2.540	1.703	2.862	2.605
	MoblieNetV2	0.601	0.567	6.909	1.195	27.345	19.532	1.195
	Resnet50	0.998	0.951	0.292	1.455	0.620	1.572	4.510
	VGG-16	0.866	0.769	2.495	3.252	3.875	4.748	2.081
Volume (cm^3)	InceptionV3	0.972	0.892	1.211	2.076	3.049	3.946	3.010
	MoblieNetV2	0.979	0.947	0.969	1.432	1.700	2.837	4.269
	Resnet50	0.998	0.957	0.284	1.259	0.691	1.532	4.748
	VGG-16	0.938	0.878	1.533	2.095	3.440	4.118	2.853

When comparing the best model from traditional ML (BME) and DL (ResNet50), it was found that the performance of the BME was as good as that of the ResNet50 in

predicting the weight of lime. On the contrary, the ResNet50 model outperformed the BME in estimating the volume of lime. In this study, BME is used as an ensemble learning technique that constructs multiple decision trees on various random subsets of the original dataset and then calculates the result by averaging their predictions. In various real-world application areas, the effectiveness of standard machine learning techniques, especially logic rule or tree-based methods, can vary greatly depending on the specific nature of the application [32]. In another way, the key benefit of DL compared to traditional ML is that it automatically learns features, eliminating the need for manual feature extraction. Deep learning independently extracts features from raw data, processes them, and makes predictions based on the extracted information [33,34]; however, DL models require large datasets for effective training, whereas traditional ML can achieve high performance with smaller datasets. From a selection perspective, DL models like ResNet50 are advantageous for tasks involving complex patterns and large datasets, such as estimating lime volume, due to their automatic feature extraction capabilities. In contrast, traditional ML models, like BME, can be more effective for smaller datasets and simpler tasks, such as predicting lime weight, where manual feature engineering is less critical. Therefore, the choice between DL and traditional ML should be guided by the dataset size and the complexity of the task at hand.

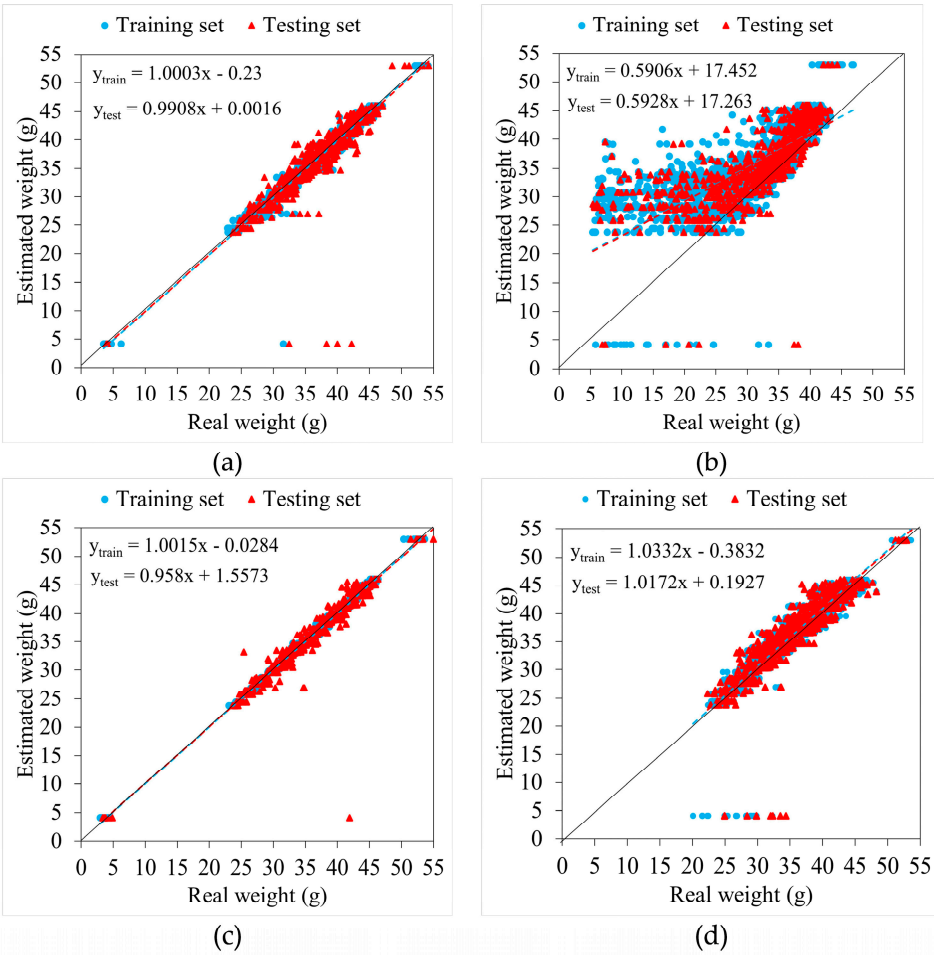

Figure 11. Scatter plots of the predicted values versus the estimated and real weights for each algorithm: (**a**) InceptionV3, (**b**) MobileNetV2, (**c**) ResNet50, and (**d**) VGG-16.

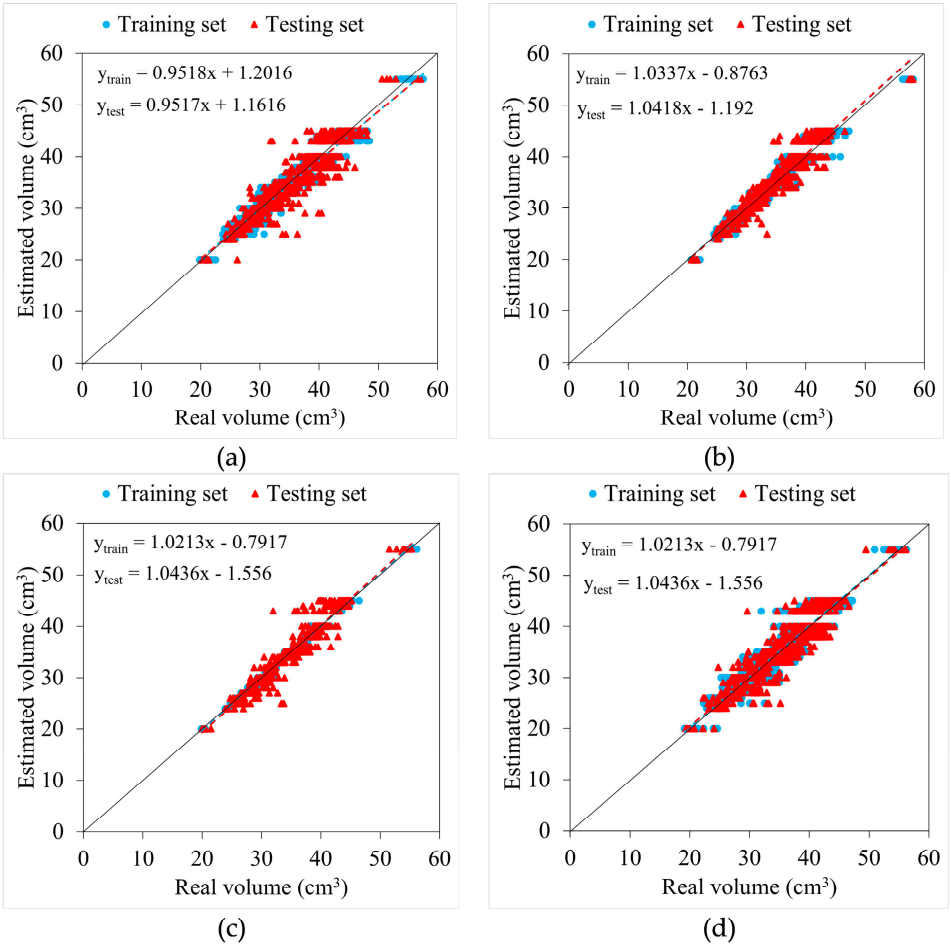

Figure 12. Scatter plots of the predicted values versus the estimated and real volumes for each algorithm: (**a**) InceptionV3, (**b**) MobileNetV2, (**c**) ResNet50, and (**d**) VGG-16.

4. Conclusions

In this study, we successfully developed and applied computer vision techniques combined with both traditional ML and DL models to estimate the weight and volume of lime fruit (*Citrus aurantifolia* (Christm.) Swingle). For traditional ML, optimal performance in terms of predicting the weight and volume of limes was obtained by BME algorithms. The R^2 values for the weight and volume of limes were 0.954 and 0.882, respectively. The automatic fine-tuning of hyperparameters in traditional ML models could significantly enhance accuracy and robustness without needing extensive computational power, offering practical alternatives for resource-constrained applications. On the contrary, ResNet50 pre-trained DL models predicted weight and volume with R^2 values of 0.951 and 0.957, respectively. The crucial advantage of DL is that the model can automatically learn and extract features from the data without requiring manual intervention, making it highly efficient for tasks with intricate patterns. The study improves the accuracy of weight and volume estimation for lime fruit, setting a new benchmark for precision in this domain. Furthermore, this study confirms that lime-packing warehouses can utilize this technique as a guideline for sizing and grading; however, these models may not yet be applicable in practice for assessing limes different (e.g., in geographic origin, harvest period, and harvest year) to those included in this study. In future studies, more robust models should be developed and validated with a large dataset representing wide variability, which would further improve the model's generalizability and practical application in real-world agricultural scenarios.

Author Contributions: Conceptualization, J.O. and R.L.; methodology, J.O. and R.L.; software, R.L.; validation, J.O., P.P. and R.L.; formal analysis, J.O., P.P. and R.L.; investigation, J.O. and R.L.; resources, J.O. and R.L.; data curation, R.L.; writing—original draft preparation, J.O. and R.L.; writing—review and editing, P.P.; visualization, R.L.; supervision, R.L.; project administration, J.O.; funding acquisition, R.L. All authors have read and agreed to the published version of the manuscript.

Funding: This work was supported by the School of Engineering, King Mongkut's Institute of Technology Ladkrabang [grant number 2567-02-01-014]. The APC was funded by the School of Engineering, King Mongkut's Institute of Technology Ladkrabang.

Data Availability Statement: The original contributions presented in the study are included in the article, further inquiries can be directed to the corresponding author.

Conflicts of Interest: The authors declare no conflicts of interest.

References

1. Beheiry, H.R.; Hasanin, M.S.; Abdelkhalek, A.; Hussein, H.A. Potassium Spraying Preharvest and Nanocoating Postharvest Improve the Quality and Extend the Storage Period for Acid Lime (*Citrus aurantifolia* Swingle) Fruits. *Plants* **2023**, *12*, 3848. [CrossRef] [PubMed]
2. Basumatary, B.; Das, P.; Nayak, P.K.; Saikia, D.; krishnan Kesavan, R. A Study on the Physical, Biochemical, Thermal and Textural Properties of Key Lime Fruit: Study on the Properties of Key Lime Fruit. *J. Sci. Ind. Res.* **2023**, *82*, 892–898.
3. Chimlek, P.; Jitanan, S. Image-based lime size grading using the comparison ratio of the pixel radius and the actual size of lime fruit. *Indones. J. Electr. Eng. Comput. Sci.* **2021**, *24*, 279–286. [CrossRef]
4. Omid, M.; Khojastehnazhand, M.; Tabatabaeefar, A. Estimating volume and mass of citrus fruits by image processing technique. *J. Food Eng.* **2010**, *100*, 315–321. [CrossRef]
5. Nyalala, I.; Okinda, C.; Chao, Q.; Mecha, P.; Korohou, T.; Yi, Z.; Nyalala, S.; Jiayu, Z.; Chao, L.; Kunjie, C. Weight and volume estimation of single and occluded tomatoes using machine vision. *Int. J. Food Prop.* **2021**, *24*, 818–832. [CrossRef]
6. Calixto, R.R.; Neto, L.G.P.; da Silveira Cavalcante, T.; Aragão, M.F.; de Oliveira Silva, E. A computer vision model development for size and weight estimation of yellow melon in the Brazilian northeast. *Sci. Hortic.* **2019**, *256*, 108521. [CrossRef]
7. Nyalala, I.; Okinda, C.; Nyalala, L.; Makange, N.; Chao, Q.; Chao, L.; Yousaf, K.; Chen, K. Tomato volume and mass estimation using computer vision and machine learning algorithms: Cherry tomato model. *J. Food Eng.* **2019**, *263*, 288–298. [CrossRef]
8. Mansuri, S.M.; Gautam, P.V.; Jain, D.; Nickhil, C. Computer vision model for estimating the mass and volume of freshly harvested Thai apple ber (*Ziziphus mauritiana* L.) and its variation with storage days. *Sci. Hortic.* **2022**, *305*, 111436. [CrossRef]
9. Sitorus, A.; Lapcharoensuk, R. A rapid method to predict type and adulteration of coconut milk by near-infrared spectroscopy combined with machine learning and chemometric tools. *Microchem. J.* **2023**, *195*, 109461. [CrossRef]
10. Yang, L.; Shami, A. On hyperparameter optimization of machine learning algorithms: Theory and practice. *Neurocomputing* **2020**, *415*, 295–316. [CrossRef]
11. Sitorus, A.; Lapcharoensuk, R. Exploring Deep Learning to Predict Coconut Milk Adulteration Using FT-NIR and Micro-NIR Spectroscopy. *Sensors* **2024**, *24*, 2362. [CrossRef] [PubMed]
12. Ismail, M.H.B.; Wagimin, M.N.; Razak, T.R. Estimating Mango Mass from RGB Image with Convolutional Neural Network. In Proceedings of the 2022 3rd International Conference on Artificial Intelligence and Data Sciences (AiDAS), Ipoh, Malaysia, 7–8 September 2022; pp. 105–110.
13. Hong, S.-J.; Kim, S.; Lee, C.; Park, S.; Kim, K.-C.; Lee, A.; Kim, G. On-plant size and weight estimation of tomato fruits using deep neural networks and RGB-D imaging. *J. ASABE* **2024**, *67*, 439–450. [CrossRef]
14. Masuda, K.; Uchida, R.; Fujita, N.; Miyamoto, Y.; Yasue, T.; Kubo, Y.; Ushijima, K.; Uchida, S.; Akagi, T. Application of deep learning diagnosis for multiple traits sorting in peach fruit. *Postharvest Biol. Technol.* **2023**, *201*, 112348. [CrossRef]
15. Naranjo-Torres, J.; Mora, M.; Hernández-García, R.; Barrientos, R.J.; Fredes, C.; Valenzuela, A. A review of convolutional neural network applied to fruit image processing. *Appl. Sci.* **2020**, *10*, 3443. [CrossRef]
16. Mohsenin, N.N. Physical Properties of Plant and Animial Materials. Vol. 1. Structure, Physical Characterisitics and Mechanical Properties; 1970; Volume 1. Available online: https://www.cabidigitallibrary.org/doi/full/10.5555/19720401916 (accessed on 16 October 2024).
17. Otsu, N. A threshold selection method from gray-level histograms. *IEEE Trans. Syst. Man Cybern.* **1979**, *9*, 62–66. [CrossRef]
18. Goceri, E. Image augmentation for deep learning based lesion classification from skin images. In Proceedings of the 2020 IEEE 4th International Conference on Image Processing, Applications and Systems (IPAS), Genova, Italy, 9–11 December 2020; pp. 144–148.
19. Khalifa, N.E.; Loey, M.; Mirjalili, S. A comprehensive survey of recent trends in deep learning for digital images augmentation. *Artif. Intell. Rev.* **2022**, *55*, 2351–2377. [CrossRef]
20. Pornchaloempong, P.; Sharma, S.; Phanomsophon, T.; Srisawat, K.; Inta, W.; Sirisomboon, P.; Prinyawiwatkul, W.; Nakawajana, N.; Lapcharoensuk, R.; Teerachaichayut, S. Non-Destructive Quality Evaluation of Tropical Fruit (Mango and Mangosteen) Purée Using Near-Infrared Spectroscopy Combined with Partial Least Squares Regression. *Agriculture* **2022**, *12*, 2060. [CrossRef]

21. Nettleton, D. Chapter 6. Selection of Variables and Factor Derivation. In *Commercial Data Mining: Processing, Analysis and Modeling for Predictive Analytics Projects*; Elsevier: Amsterdam, The Netherlands, 2014; pp. 79–104.
22. Williams, P.; Antoniszyn, J.; Manley, M. *Near Infrared Technology: Getting the Best out of Light*, 1st ed.; African Sun Media: Stellenbosch, South Africa, 2019.
23. Basak, J.K.; Paudel, B.; Kim, N.E.; Deb, N.C.; Kaushalya Madhavi, B.G.; Kim, H.T. Non-Destructive Estimation of Fruit Weight of Strawberry Using Machine Learning Models. *Agronomy* **2022**, *12*, 2487. [CrossRef]
24. Lee, D.H.; Cho, Y.; Choi, J.M. Strawberry volume estimation using smartphone image processing. *Hortic. Sci. Technol.* **2017**, *35*, 707–716. [CrossRef]
25. Sharma, R.; Kumar, M.; Alam, M. Image processing techniques to estimate weight and morphological parameters for selected wheat refractions. *Sci. Rep.* **2021**, *11*, 20953. [CrossRef]
26. Wang, H.; Xiong, J.; Li, Z.; Deng, J.; Zou, X. Potato grading method of weight and shape based on imaging characteristics parameters in machine vision system. *Trans. Chin. Soc. Agric. Eng.* **2016**, *32*, 272–277.
27. Biancolillo, A.; Næs, T. The sequential and orthogonalized PLS regression for multiblock regression: Theory, examples, and extensions. In *Data Handling in Science and Technology*; Elsevier: Amsterdam, The Netherlands, 2019; Volume 31, pp. 157–177.
28. Radovich, T.J.; Kleinhenz, M.D. Rapid estimation of cabbage head volume across a population varying in head shape: A test of two geometric formulae. *HortTechnology* **2004**, *14*, 388–391. [CrossRef]
29. Demirsoy, H.; Demirsoy, L. Prediction model for estimating peach fruit weight and volume on the basis of fruit linear measurements during growth. *J. Fruit Ornam. Plant Res.* **2007**, *15*, 65.
30. Bozokalfa, M.K.; Kilic, M. Mathematical modeling in the estimation of pepper (*Capsicum annuum* L.) fruit volume. *Chil. J. Agric. Res.* **2010**, *70*, 626–632. [CrossRef]
31. Edalatifar, M.; Tavakoli, M.B.; Ghalambaz, M.; Setoudeh, F. Using deep learning to learn physics of conduction heat transfer. *J. Therm. Anal. Calorim.* **2021**, *146*, 1435–1452. [CrossRef]
32. Sarker, I.H. Deep learning: A comprehensive overview on techniques, taxonomy, applications and research directions. *SN Comput. Sci.* **2021**, *2*, 420. [CrossRef]
33. Chauhan, N.K.; Singh, K. A review on conventional machine learning vs deep learning. In Proceedings of the 2018 International Conference on Computing, Power and Communication Technologies (GUCON), Greater Noida, India, 28–29 September 2018; pp. 347–352.
34. Gencturk, B.; Arsoy, S.; Taspinar, Y.S.; Cinar, I.; Kursun, R.; Yasin, E.T.; Koklu, M. Detection of hazelnut varieties and development of mobile application with CNN data fusion feature reduction-based models. *Eur. Food Res. Technol.* **2024**, *250*, 97–110. [CrossRef]